

Comparison of Signals from South and West VLF Stations During June 2021

Whitham D. Reeve

1. Introduction

It is known that the solar terminator (gray line) and other diurnal variations in the spherical earth-ionosphere waveguide affect VLF propagation. Plots over time of the signal power received from distant VLF transmitters have a characteristic pattern and are used to verify receiver and antenna operation and the receiver noise environment and to detect sudden ionospheric disturbances (SID) and other effects associated with solar flares.

The signals propagate along what are known as *short* and *long* paths. The short path is the most direct great circle path between the transmitter and receiver, and it involves one or, possibly, more waveguide modes depending on its length and other conditions. On the other hand, the long path usually is not a single, simple great circle path but is much more complicated because of its greater length, possible non-great circle routing over Earth's surface and mode changes at land, water, and ice interfaces. The various paths and waveguide modes may interfere with each other, both constructively and destructively. Thus, variations may exist in the received signal levels due not only to diurnal solar effects but also to propagation path characteristics. For more information on VLF propagation, see [{Reeve19-1}](#)

To investigate these effects, I recorded the received signal levels on two disparate propagation paths, one from a VLF transmitter located south of Coho Radio Observatory (CRO) and another from a VLF transmitter located west of CRO (figure 1). Both paths are predominantly over water. Data were recorded during two separate sessions in June 2021. It is shown that the daily signal variations for the south path are significantly different than the west path. While that is not surprising, the data form the basis for further study. Also, it happened that during data collection on the south path, an annular solar eclipse occurred on 10 June. The eclipse was not visible from the path being recorded that day; however, eclipses are known to affect VLF propagation so the characteristics of the data plot for that date are briefly analyzed.

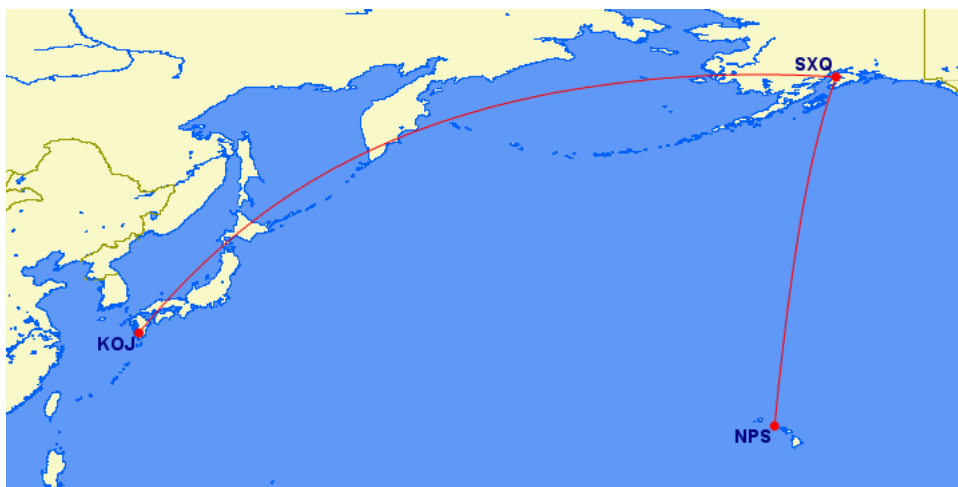


Figure 1 ~ Short paths from Hawaii and Japan to Coho Radio Observatory in Alaska. For path mapping purposes, the end points are indicated by the nearest airports: SXQ (Soldotna Municipal Airport near CRO), KOJ (Kagoshima Airport near the JJI transmitter location) and NPS (Ford Island NALF Airport near the NPM transmitter location). Image source: Great Circle Mapper [{GCM}](#)

In the case of the south transmitter station, NPM in Hawaii, the solar terminator crossed the short propagation path twice each day at a sharp angle during the times investigated. For the west station, JJI in Japan, the short

and long propagation paths and terminator vary from almost parallel to crossing at wide angles. The signal level measurements for the two transmitter stations and solar terminator maps are detailed in section 2 with additional discussion of this and future work in section 3. Instrumentation is described in section 4 and references and weblinks are listed in section 5.

2. Measurements

The information below includes signal level plots and maps showing both the short and long propagation paths. The long path, as shown, is idealized and may not be the actual VLF propagation path in the spherical waveguide but it is sufficient for visualization.

NPM → CRO summary of characteristics:

Transmitter station name, frequency and coordinates: NPM, 21.4 kHz, 21° 25' 13.38"N, 158° 09' 14.35"W

Nearest town: Lualualei, Oahu, Hawaii USA

Relative location: South of CRO

Short/long path distance and direction from CRO to NPM: 4364/35 660 km, Azimuth 190° True

Receiver antenna azimuth setting: 000°/180° True

Dates observed: 03 – 13 June 2021

The following discussion is focused on one day, 10 June; all other days were similar. As the solar terminator (figure 2) marched west on 10 June, it intersected NPM with sunset at 0521 UTC (7:21 pm local Hawaii) and then CRO with sunset at 0729 (11:29 pm local Alaska). The next sunrise at CRO was 1238 UTC (4:38 am local Alaska) followed by NPM at 1555 UTC (5:55 am local Hawaii). Since the measurements were near the summer equinox, the sunrise and sunset times varied by only about 1 minute throughout the study period. These sunrise and sunset times are at ground level and would be slightly different for the upper boundary of the earth-ionosphere waveguide, which can vary from approximately 60 to 90 km altitude.

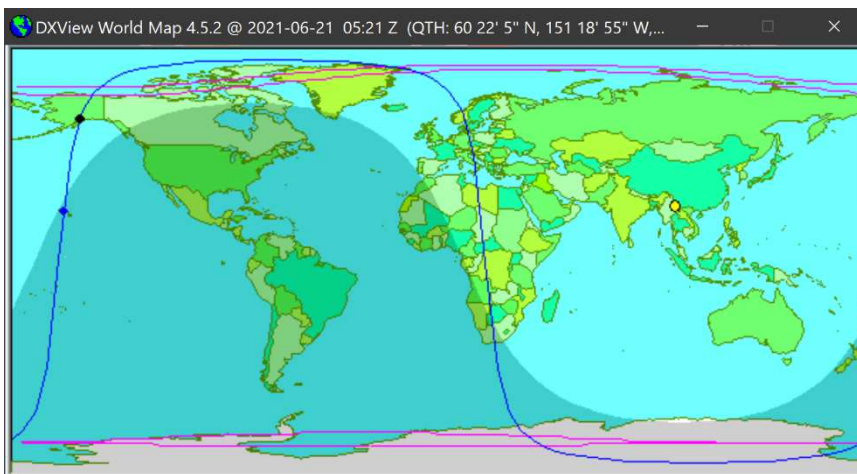


Figure 2 ~ Solar terminator and propagation paths (blue line) at 0521 UTC on 10 June when the Sun rises at station NPM. The receiver and transmitter stations are marked by small solid black circles (left side of image) and the Sun is the small solid yellow circle to the east in the middle of the daylit area. The shaded area, which indicates darkness, moves right-to-left as the day progresses. Image from DXView.

A plot of the received signal levels for the full 10-day study period (figure 3) shows a textbook repeating pattern. The received signal levels increase at night due to more favorable propagation conditions and then fall during the day as D-region absorption increases the propagation losses. Also, there are sunset and sunrise dips in the

signal levels (figure 4) as the solar terminator crosses the path. However, in this case, there are two dips at sunrise. The two dips occur 1 hour apart at about 1400 and 1500 UTC, and fall between sunrise at CRO and sunrise at NPM.

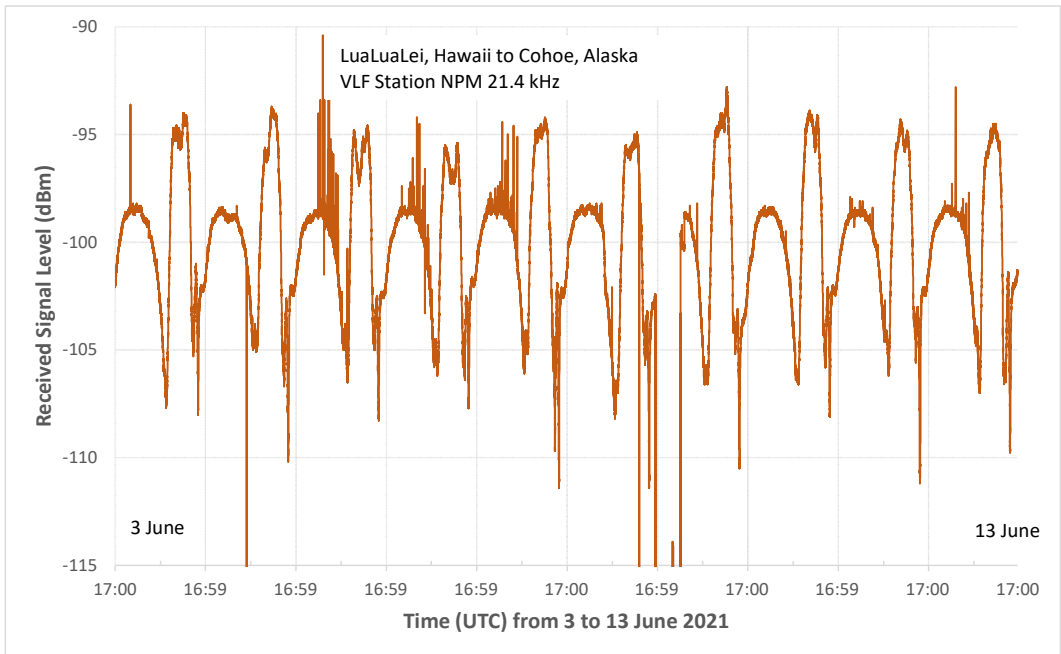


Figure 3 ~ Received signal level at CRO for the 10-day period between 3 and 13 June 2021 from station NPM in Hawaii. Note the short signal dropout on 4 June and a longer dropout on 9 June. These probably are due to transmitter maintenance or failures. There were no known receiver problems.

Another interesting phenomenon is the signal level dip at about 1045 UTC, at which time both the transmit and receive stations and the short path were in darkness (figure 5). However, the Sun was directly over the long path, and the dip may be due to destructive interference between the short and long paths at the receiver. Examination of the data for each of the 10 days shows that the dip does not appear every night.

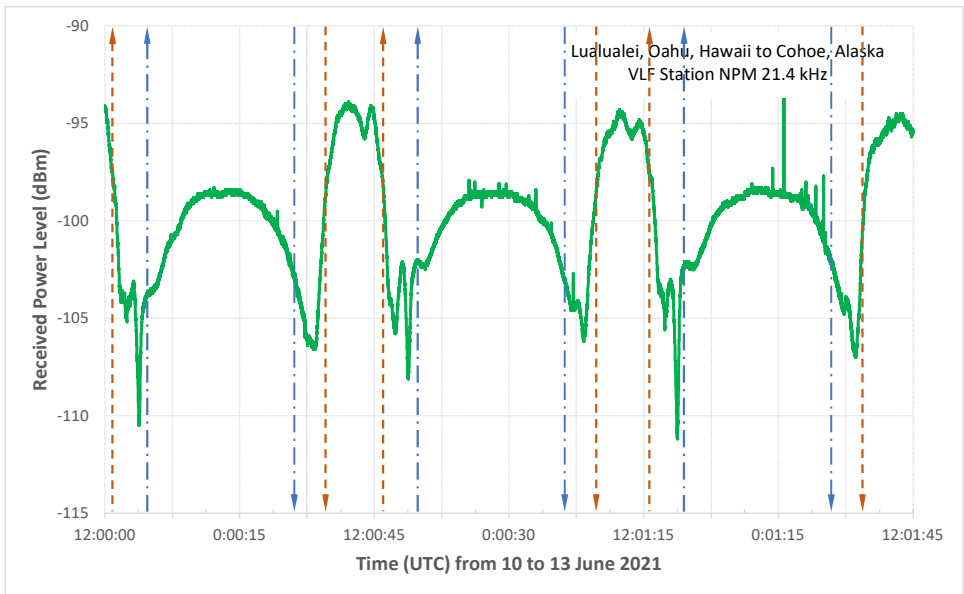


Figure 4 ~ Plot of received signal level for the 3-day period from 10 to 13 June 2021 on the path from NPM to CRO. The repeating pattern is caused by varying propagation conditions during each day and night. The dashed arrowed lines indicate sunset (down arrows) and sunrise (up arrows). The blue lines are for the VLF transmitter at NPM and the orange lines are for the receiver at CRO.

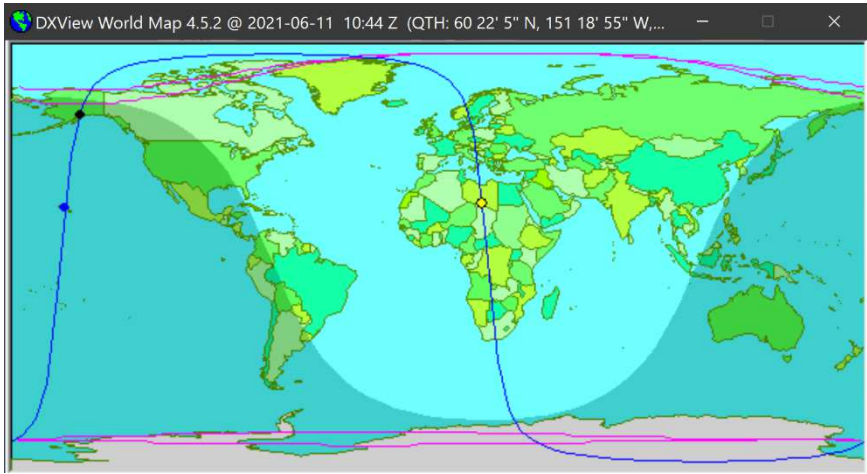
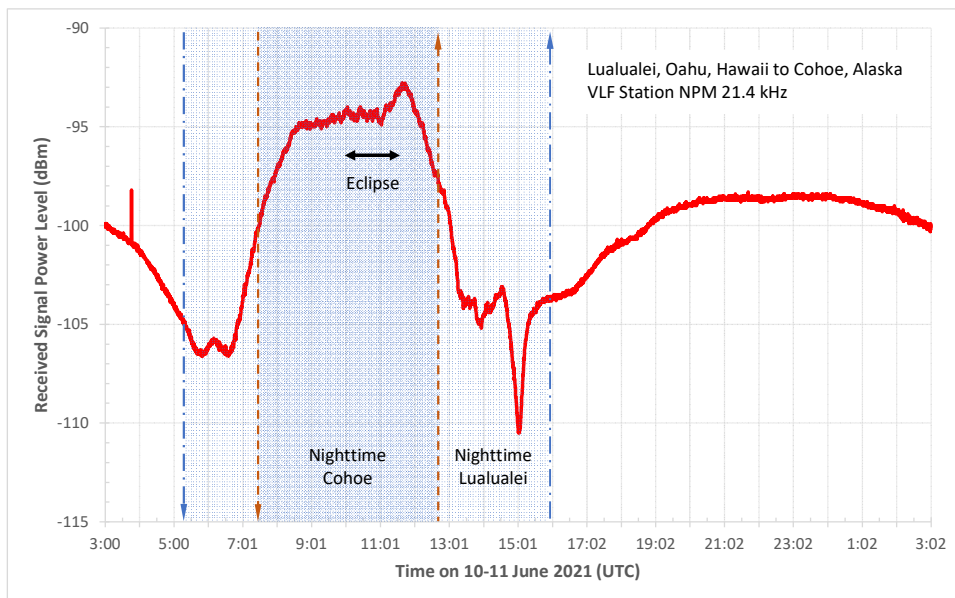
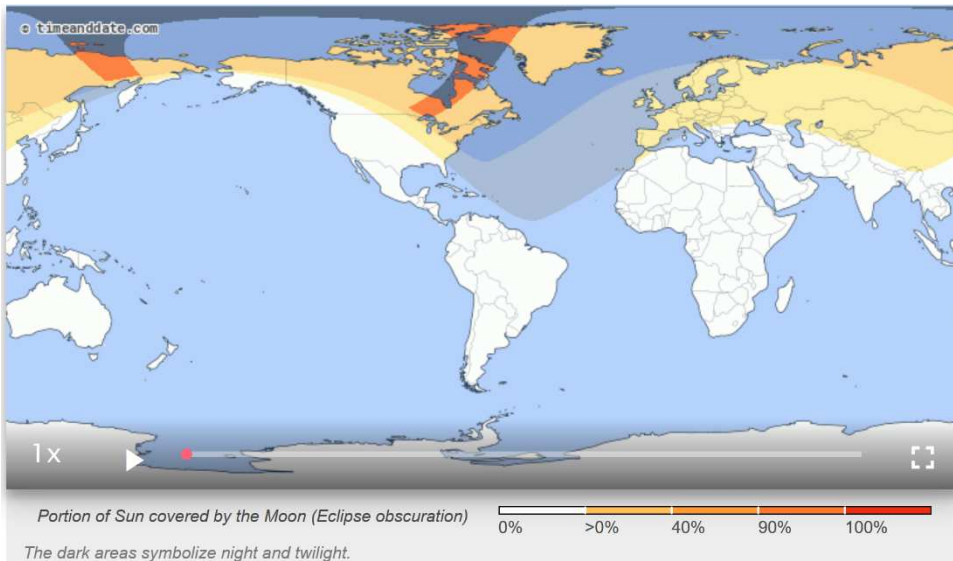


Figure 5 ~ Short and long paths between NPM and CRO (blue line) with solar terminator at 1045 UTC on 11 June 2021, corresponding to the time of the dip seen in the received signal level plot for 11 and 12 June. Image from DXView

Solar eclipse: The solar eclipse on 10 June occurred while the NPM transmitter and CRO receiver locations and short path were in darkness. However, the eclipse annularity path as well as the broader path of the partially eclipsed Sun (figure 6) crossed the long propagation path. Signal level plots for the days before and after the eclipse appear similar to eclipse day (figure 7), but the signal peak near 1200 UTC on 10 June has a slightly higher level than the same time on other days (table 1). This may be unrelated to the eclipse but worth noting.

Table 1 ~ Measured peak signal level during each day near 1200 UTC. Note that the level on eclipse day 10 June is higher than any other day and about 2 dB higher than the average of all other days.

Date	Peak level (dBm)	Remarks
4 June	-94.2	
5 June	-94.3	
6 June	-94.7	
7 June	-95.4	
8 June	-94.6	
9 June	-95.1	
10 June	-92.9	Eclipse day
11 June	-94.3	
12 June	-95.0	
13 June	-95.6	
Average	-94.8	All days except 10 June
Std Dev	0.48	All days except 10 June



JJI → CRO summary of characteristics:

Transmitter station name, frequency and coordinates: JJI, 22.2 kHz, 32° 04' 58"N, 130° 49' 33"E

Nearest town: Ebino, Miyazaki, Japan

Relative location: West of CRO

Short/long path distance and direction from CRO to JJI: 6299/33 725 km, azimuth 277° True

Receiver antenna azimuth setting: 090°/270° True

Dates observed: 14 – 24 June 2021

The propagation conditions from the VLF station JJI near Ebino in Japan are quite different from the station in Hawaii in that, at times, the solar terminator is almost parallel to the propagation path and other times crosses the short and long paths at wide angles (figure 8). The sunrise and sunset times for 21 June are 1236 and 0737 UTC (4:36 am and 11:37 pm local Alaska) at CRO and 2011 and 1026 UTC (5:11 am and 7:26 pm local Ebino) at

JJI, respectively. Note that, as with the NPM path, these sunrise and sunset times vary by only about 1 minute throughout the 10-day study period.

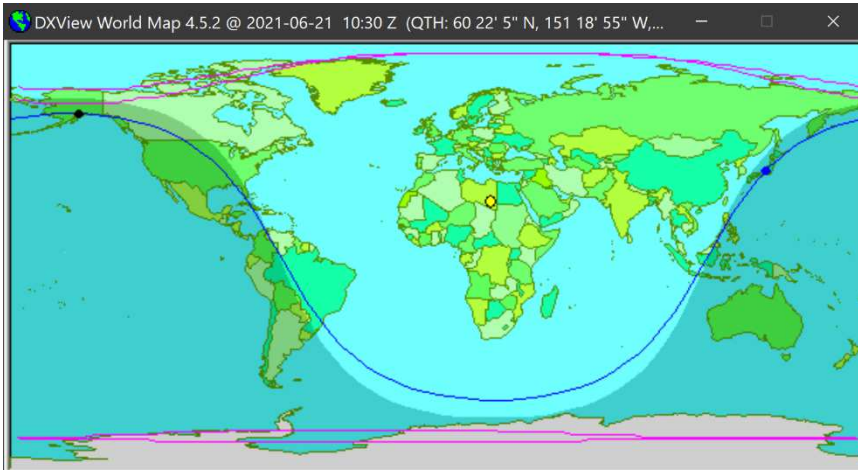


Figure 8.a ~ Solar terminator for the JJI to CRO path at 1030 UTC on 21 June on the path from the west station JJI to CRO. The terminator and great circle propagation paths (blue line) are very close to the same at the time shown. Image from DXView.

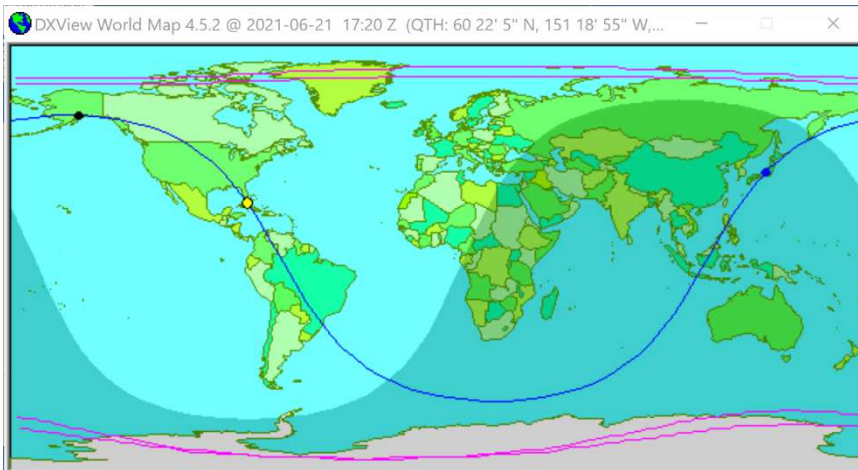


Figure 8.b ~ Solar terminator for the JJI to CRO path at 1720 UTC on 21 June, 7 hours later than the previous image. At the time shown, the solar terminator crosses the short path at nearly a right angle and the Sun is directly over the long path. Image from DXView.

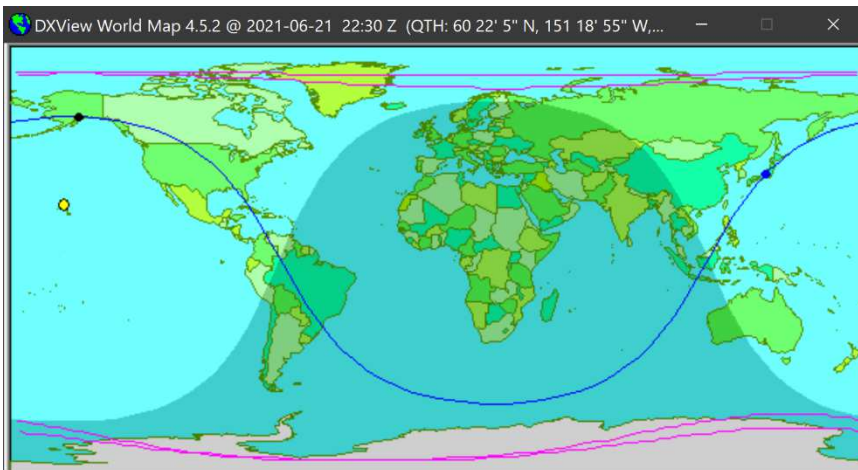


Figure 8.c ~ Solar terminator for the JJI to CRO path at 2230 UTC on 21 June, 5 hours later than the previous image. At the time shown, the solar terminator crosses the long propagation path twice at wide angles. Image from DXView.

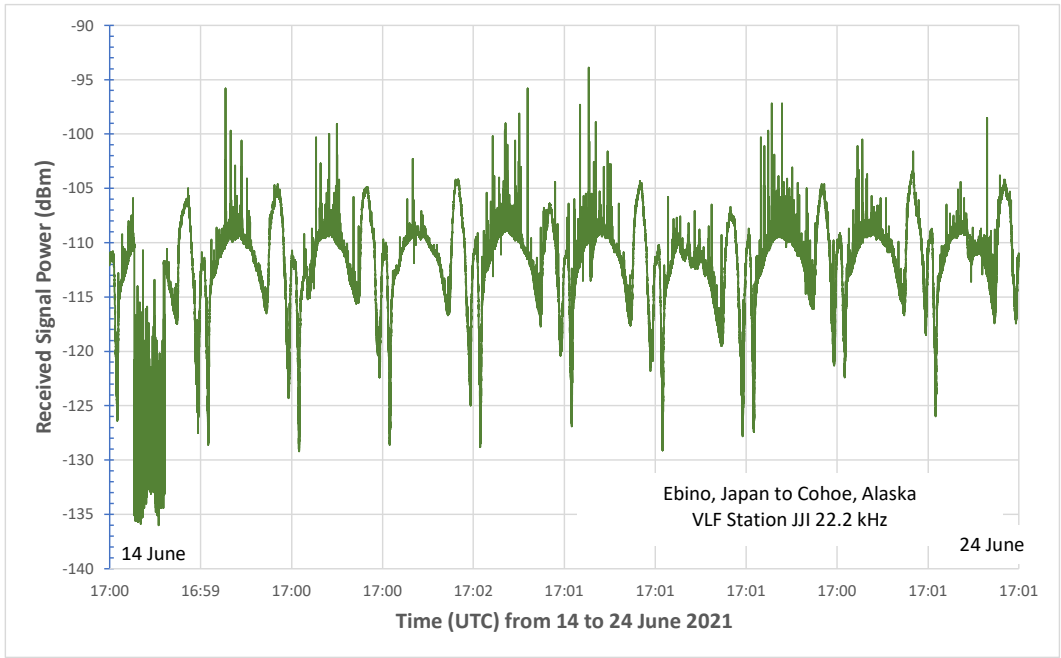


Figure 9 ~ Received signal level at CRO for the 10-day period between 14 and 24 June 2021 from VLF station JJI in Japan. The peak signal levels are about 10 dB lower compared to the NPM path and the daily pattern is different but still recognizable as VLF propagation.

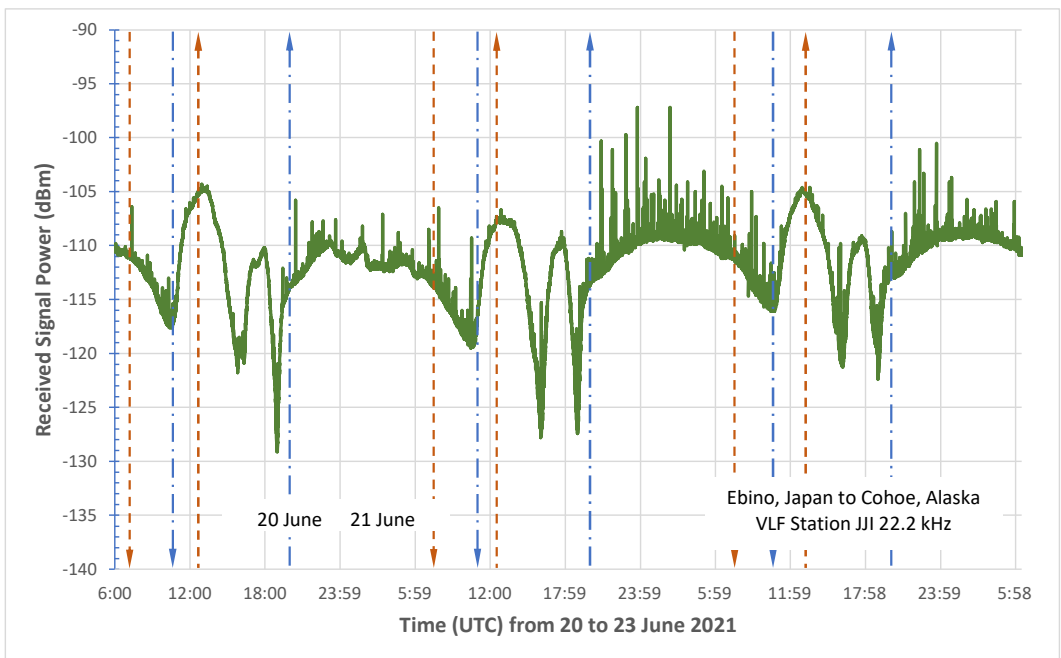


Figure 10 ~ Plot of received signal level for the 3-day period from 20 to 23 June 2021 on the path from JJI to CRO. The dashed arrowed lines indicate sunset (down arrows) and sunrise (up arrows). The blue lines are for the VLF transmitter at JJI and the orange lines are for the receiver at CRO. Note the noise increase between sunrise and sunset at the transmitter station.

The signal level plot for a single 24-hour period on the JJI to CRO circuit shows two signal peaks and three dips that are quite different than those seen on the NPM to CRO circuit (figure 11). On the NPM to CRO circuit, the nighttime signal power has a small dip as previously explained. On the other hand, on the JJI to CRO circuit, there are two substantial peaks and two dips that occur during darkness at JJI. The first dip near 1030 UTC corresponds to when the solar terminator is almost parallel with both the short and long propagation paths; the time is coincident with sunset at JJI. The first peak near 1300 UTC is close to sunrise at CRO. The second dip near 1600 UTC occurs about 1 hour before the Sun crosses the long propagation path. At that time, the terminator crosses both the short and long paths about midway along their lengths. The second peak near 1800 UTC occurs

about 1 hour after the Sun crosses the long propagation path. Finally, the third dip near 1900 UTC occurs just before sunrise at JJI.

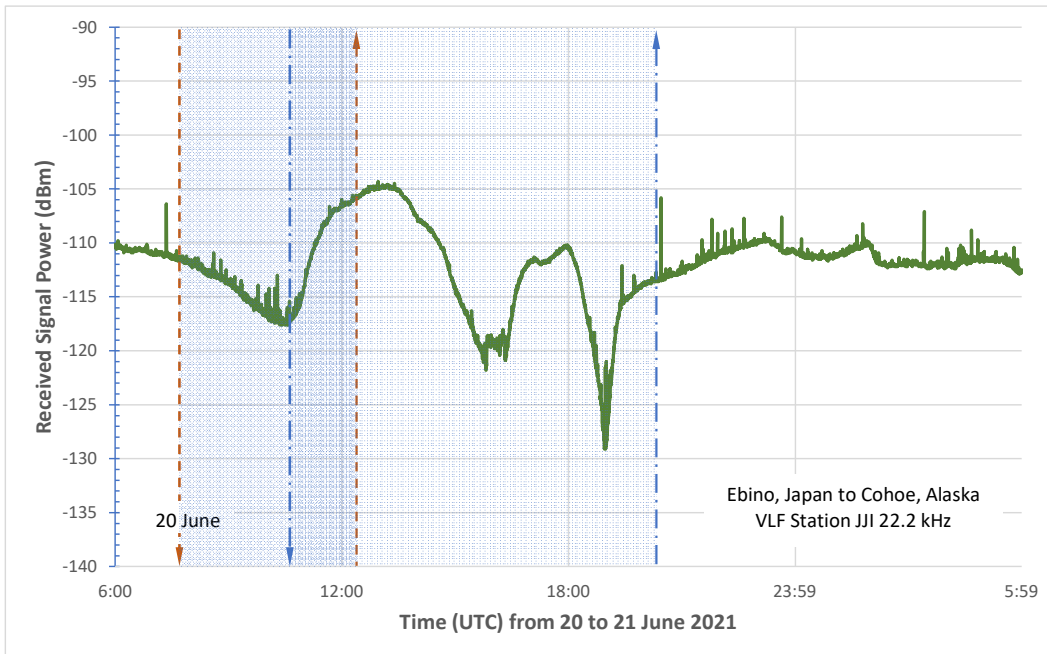


Figure 11 ~ Plot of received signal level on the path from JJI to CRO for the 24-hour period from 0600 UTC on 20 June to 0600 on 21 June 2021. The dashed arrowed lines and shaded area are the same as in previous plots. See text for timing of the various signal peak and dip features.

3. Discussion & Future Work

The data represents only two radio circuits recorded near the summer equinox. The path from the west Japanese station is longer than the path from the south Hawaiian station by almost 2000 km and the received signal levels were about 10 dB lower. The repeating signal level patterns for the two paths during the study periods showed significant differences.

At least some of the pattern differences were due to the interaction of the paths with the varying ionization associated with the solar terminator and other daily variations that normally occur on north-south as opposed to east-west propagation paths. Magnetic field variations and disturbances will affect propagation but this aspect has not been explored. There may be evidence of short and long path interference on the circuits.

For future work, the signal variations from VLF stations to the north and east of CRO will be investigated. The signals from any north station would propagate over land and the North Pole or Greenland (and ice) as opposed to the south overwater path from Hawaii. Similarly, the propagation from some east stations would follow overland paths as opposed to the west overwater path from Japan.

Another factor that is known to affect VLF propagation and will be studied are the effects on specific propagation paths by the solar cycle progression. At the time of this writing, solar cycle 25 has been underway for 1½ years. Recording signal level data on the same two paths every six months or one year throughout the cycle likely would reveal any long-term changes.

Finally, although the solar eclipse on 10 June produced no verifiable indications on the NPM to CRO path, future eclipses are worth monitoring. A little online research quickly reveals what, when and where VLF propagation paths will be crossed by an eclipse path over the next few years. For example, a good place to start is [NASA](#).

3. Instrumentation

The CRO receiver station is located at 60°22'4.68"N, 151°18'55.14"W. A shop-built square loop antenna and SDRPlay *RSPduo* software defined radio (SDR) receiver are used for VLF work. *SDRuno* software, which is native to the SDRPlay SDR products, was used to gather reception data. A block diagram shows the basic setup (figure 12). More details are given at [Reeve19-2](#).

The *PWR & SNR to CSV* function in *SDRuno* was used to save the measured signal level every 15 seconds to Comma Separated Variable (.csv) files over the two 10-day study periods. Excel was then used to plot the data for various time periods as seen in the previous section.

The main spectrum and waterfall displayed by *SDRuno* shows all received signals within the configured bandwidth. For the measurements discussed in this article the receiver was set to Zero Intermediate Frequency (ZIF) mode with a sample rate of 2 MHz and factor 8 decimation. These settings provide 250 kHz maximum displayed bandwidth. I used the zoom function to reduce the displayed range to 10 to 40 kHz with 3.81 Hz resolution (FFT bin size of 65 536) (figure 13). The receiver IF gain was set to Auto. The RF gain was adjusted to provide the best signal-to-noise ratio on each of the paths.

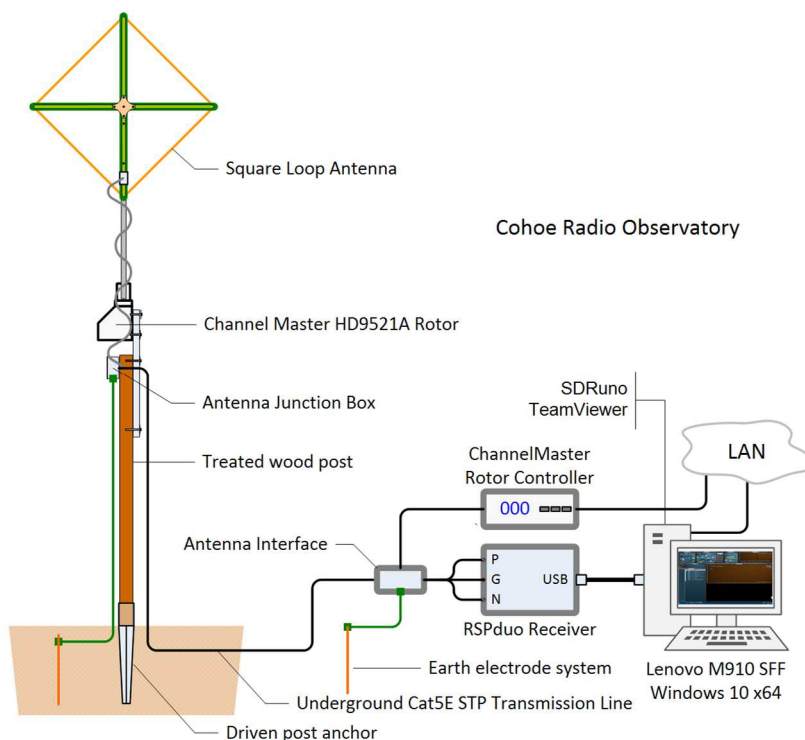


Figure 12 ~ Block diagram of Cohoe Radio Observatory VLF receiver and antenna setup. The diagonal dimension of the loop antenna is 1.2 m and its center is 3.5 m above ground level. The balanced high-impedance (HI-Z) antenna input of the receiver is connected to the antenna through Cat5E STP DB (direct burial) cable. The rotor controller has been modified to enable control over the local area network. Image © 2021 W. reeve

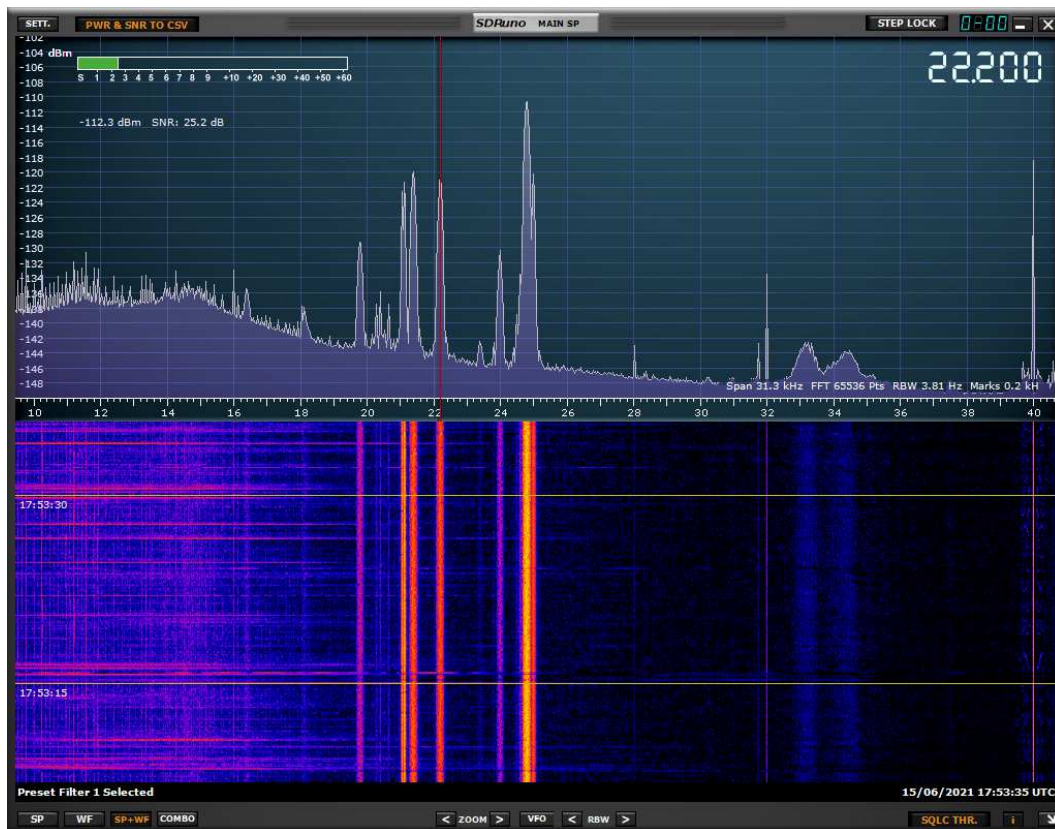


Figure 13 ~ Spectrum and waterfall for 15 June 2021 showing receiver tuned to the JJI station on 22.2 kHz (marked by the red vertical line in the upper panel). The loop antenna was oriented east-west. Many VLF signals are present including NPM to the south. The strongest signal is station NLK in Washington USA to the east at 24.8 kHz. Other identified signals are (with presumed station name in parentheses): 16.4 (JXN), 18.1 (RDL), 21.1 (RDL), 21.4 (NPM), 23.4 (DHO38), 24.0 (NAA), 24.8 (NLK), and possibly 25.0 and 31.9 kHz. There may be an additional signal at 24.6 kHz hidden behind the strong signal at 24.8 kHz. The very narrow spectrum spikes seen at 16, 32 and 40 kHz are spurious signals at 8 kHz intervals; the spike at 24 kHz is hidden by a signal. The wide double-hump signal at 33-34 kHz is unknown and not visible with the antenna pointed north-south.

5. References & Weblinks

- {Reeve19-1} Reeve, W., Monitoring Low Frequency Propagation with a Software Defined Radio Receiver, Part I ~ Concepts, 2020, available at:
http://www.reeve.com/Documents/Articles%20Papers/Propagation/Reeve_LFProp-ConceptsP1.pdf
- {Reeve19-2} Reeve, W., Monitoring Low Frequency Propagation with a Software Defined Radio Receiver, Part II ~ Observations, 2019, available at:
http://www.reeve.com/Documents/Articles%20Papers/Propagation/Reeve_LFProp-ObsvP2.pdf
- {GCM} <http://www.gcmapp.com/mapui?P=NPS-SXQ-KOJ>
- {NASA} <https://eclipse.gsfc.nasa.gov/SEgoogle/SEgoogle2021.html>
- {TimeDate} <https://www.timeanddate.com/eclipse/solar/2021-june-10>



Author: Whitham Reeve obtained B.S. and M.S. degrees in Electrical Engineering at University of Alaska Fairbanks, USA. He worked as a professional engineer and engineering firm owner/operator in the airline and telecommunications industries for more than 40 years and now manufactures electronic equipment used in radio astronomy. He also is a part-time space weather advisor for the High-frequency Active Auroral Research Program (HAARP) and a member of the HAARP Advisory Committee. He has lived in Anchorage, Alaska his entire life. Email contact: whitreeve@gmail.com
